



Zn²⁺ Influence on Optical and Structural Properties of Nano composite Materials: Optical Communications

Sharanappa Chapi^{*,**} and H. Devendrappa^{*}

^{*}Department of Physics, Mangalore University, Mangalagangothri, Karnataka - 574 199, INDIA

^{**}Department of Physics, Jagadguru Tontadarya College, Gadag-Betgeri, Karnataka – 582 101, INDIA

(Corresponding author: Sharanappa Chapi)

(Received 16 September, 2016 Accepted 19 October, 2016)

(Published by Research Trend, Website: www.researchtrend.net)

ABSTRACT: Polymer nanocomposites (PNCs) film doped with ZnO-NPs was prepared by spin-coating method. Firstly, ZnO NPs were synthesized by Co-precipitation method. The X-Ray diffraction (XRD) analysis revealed that the synthesized ZnO NPs have the pure wurtzite structure. The crystalline sizes were estimated by the Debye Scherer's formula and values were in good agreement with the TEM analysis. Morphology index, Lorentz factor and Lorentz polarization factor were also studied. The optical properties of all films were investigated using spectrophotometric (UV-Vis) measurement of transmittance $T(\lambda)$ in the wavelength range 200-800 nm. The optical transmission method is successfully used to determine the absorption coefficient (α), forbidden energy gap (E_g) and skin depth. The real and imaginary parts of the dielectric constants ϵ_r and ϵ_i are calculated from which the volume energy loss function, the surface energy loss function were deduced. The variation in film morphology was examined by scanning electron microscopy (SEM). The study reveals that all these parameters are affected by the increase in the percentage of ZnO NPs. These obtained results suggest that the polymer blend electrolytes are suitable candidatures for various applications in electronic and optical devices.

Keywords: Doped-ZnO, Spin-Coat, XRD, Optical parameters, Optical band gaps,

I. INTRODUCTION

Solid polymer electrolytes have attracted attention for more than three decades because of their practical applications as well as for their fundamental knowledge. Polymer blends have important contemporary ways for the development of new polymeric materials with desirable properties for wide variety of potential applications as solid state batteries in computers, mobile phones, electric vehicles, opto-electronic devices etc [1-3].

PEO is still an active candidate for polymer electrolytes [4] because of its good salivation power, having a single helical structure which supports the fast ionic conduction and many physicochemical properties but its practical applications are limited because of semicrystalline nature of PEO at room temperature. It is reported by Radhakrishnan *et al.* [5] that crystallization of PEO can be controlled by its blending with amorphous polymer. Polymer blending is one of the effective methods to reduce crystalline content and enhance the amorphous content. Polyblends often exhibit properties that are superior to the individual component polymers [6].

Hence, we have added poly(vinyl pyrrolidone) (PVP) as other polymer because PVP is an amorphous polymer and it has drawn special attention amongst the conjugated polymers. It has good environmental stability, easy process situation and excellent transparency. PVP is a potential material having a good charge storage capacity and optical properties. Chemically PVP has been found to be inert, nontoxic and interestingly, it displays a strong tendency for complex formation with a wide variety of smaller molecules [2, 7].

Nanocomposites (NCs) are a class of high-performance novel materials containing polymer and nanoparticles (NPs). In recent years, many researchers have successfully synthesized NCs by incorporating different NPs into a organic matrix.

ZnO can be considered as an "old" semiconductor which has attracted researcher's attention for a long time because of its large area of applications. ZnO is a direct band gap semiconductor with $E_g = 3.37$ eV (at room temperature) having hexagonal structure with lattice parameters $a = 0.325$ nm and $c = 0.512$ nm [8].

However, to the best of the author's knowledge, no work is reported on blended PEO/PVP with ZnO NPs as dopant. In this investigation, we have made an attempt to prepare PEO/PVP/ZnO based electrolytes with different concentrations of ZnO NPs by spin-coat technique.

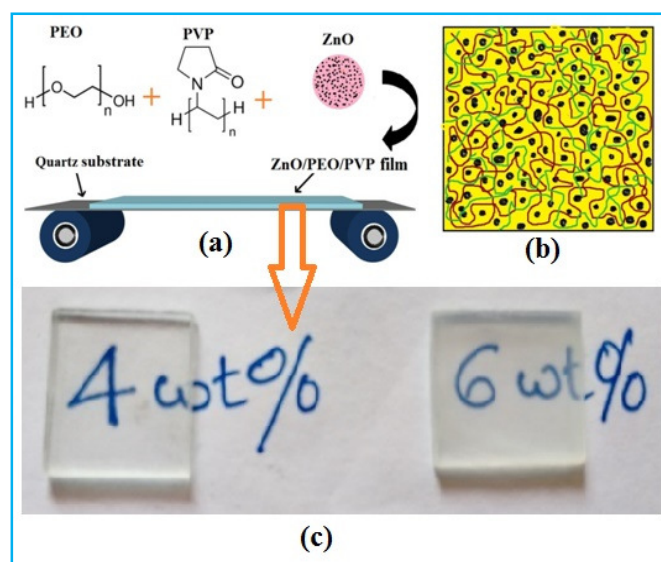
II. EXPERIMENTAL

Materials and synthesis of ZnO nanoparticles. Polyethylene oxide ($M_w = 5 \times 10^6$) and polyvinylpyrrolidone ($M_w = 4 \times 10^4$) purchased from Sigma Aldrich, chloroform ($M_w = 119.38$) obtained from Himedia was used as common solvent for both polymers. Sodium hydroxide (NaOH), zinc nitrate hexahydrate ($Zn(NO_3)_2 \cdot 6H_2O$), double distilled water were used for synthesis of ZnO nanoparticles with the help of Co-precipitation method. In the synthesis, 50 ml of 1M concentration sodium hydroxide (NaOH) was added drop wise to a conical flask containing 100 ml of 0.1M concentration of $Zn(NO_3)_2 \cdot 6H_2O$ at room temperature. The obtained solution was centrifuge and the obtained powder was washed with double distilled water for 5-6 times. The powder was dried in hot air oven at 120 °C for 8 h to get ZnO nanopowder.

Preparation and characterization of PEO/PVP-ZnO. PEO/PVP and synthesized ZnO NPs

(PEO/PVP/ZnO) were prepared in weight ratios (50/50/0), (48/48/4) and (47/47/6) by spin-coat (Model VTC-100) method [7] over quartz substrates which were cleaned by toluene. PEO/PVP and ZnO NPs were separately dissolved in chloroform at room temperature. The nano-polymer matrix was stirred well for 10-12 h for homogeneous mixing with the help of magnetic stirrer. The mixture was injected on substrate and the spin-coating machine was set at 2500 rpm for 20 s (T_1) and 4000 rpm for 40 s (T_2) followed by solvent-drying for 10 min. The finally obtained uniform NCs film is as shown in Scheme 1(a). The possible interaction of the Zn^{2+} ion concentration and its effect on PEO/PVP system is as shown in scheme 1(b). Scheme 1(c) shows, the digital camera image of highly transparent spin-coated PNCs (4 and 6 wt% of ZnO NP) film.

The obtained PNCs were characterized by X-ray diffraction with $CuK\alpha$ radiations ($\lambda=1.5418\text{\AA}$) in the 2θ range of $10-80^\circ$ with a scan rate of 5° min^{-1} . The optical reflectance data was carried out in the wavelength range of 200-1100 nm using double beam Phakin-Elmer Lambda 35 (USA) spectrophotometer. Transmission electron microscopy (TEM) and scanning electron microscopy (SEM, Sigma Zeiss, Carlzeish) images of the films were also taken.



Scheme-1: (a) Molecular structure of PEO, PVP and its ZnO NCs film on quartz substrate, (b) Possible interaction of polymer matrix; PEO (red curves) PVP (green curves), the black points indicates the ZnO NPs and, (c) Digital camera image of highly transparent spin-coated 4 and 6 wt% doped PNC films.

III. RESULTS AND DISCUSSION

TEM analysis of ZnO nanoparticles. Figure 1 represents the transmission electron microscopy (TEM) micrograph of the ZnO NPs. It clearly exhibits a growth of ZnO particles.

However the diameter of these particles is not uniform; the average size of the particles is about 35-50 nm in diameter. The figure clearly indicates the morphology of the particles (roughly) spherical in shape and homogenous.

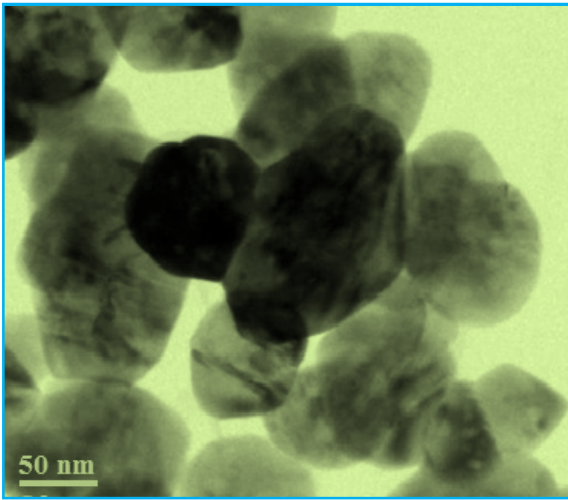


Fig. 1. TEM images of the as-prepared ZnO NPs.

XRD analysis. The XRD patterns of pure ZnO NPs and 6 wt% nanocomposite polymer electrolyte (NCPE) complexes as shown in Fig. 2(a) and (b) respectively. The diffraction peaks located around $2\theta \sim 19^\circ$ and 23° in the complexes are associated to the characteristics peak of PEO/PVP. The new lowest diffraction peaks appears at 31.8° , 34.4° , 36.2° , 47.5° and 56.7° corresponding to (100), (002), (101), (102) and (110) planes. This is good agreement with the JCPDS file no. 80-0074 and is indexed as the hexagonal wurtzite structure of ZnO (Fig. 2c) having space group P63mc and are consistent with the crystal structure similar value has also been reported [9].

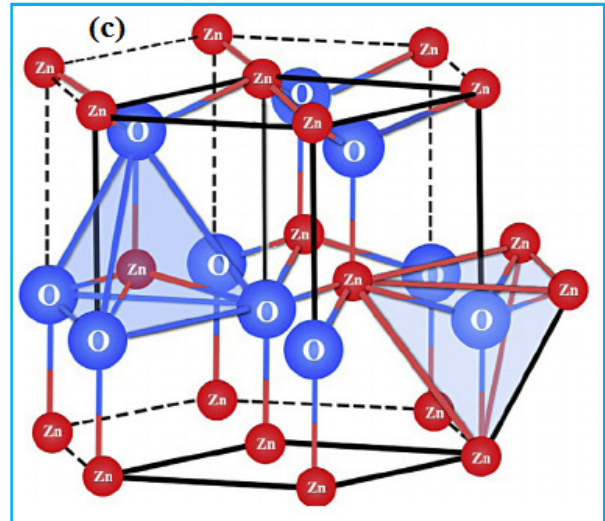
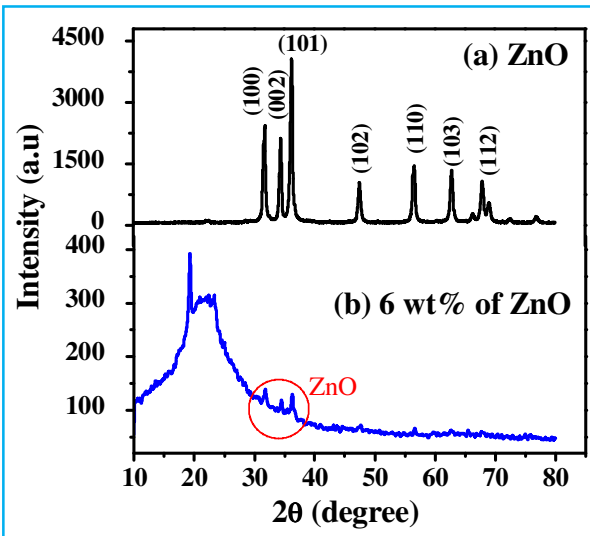


Fig. 2. X-ray diffraction of (a) ZnO NPs, (b) PEO/PVP/ZnO (47:47:6) PNCs and (c) Schematic diagram of the wurtzite structure of ZnO.

The crystalline phase in PEO/PVP blend matrix is reduced on addition of Zn^{2+} as shown in Fig. 2(b). This may due to the coordination and interactions between the Zn^{2+} ion and other oxygen atoms of polymer chain. The Scherer formula for the maximum peak of pure ZnO and 6 wt% PNCs electrolyte is used to determine the crystallites sizes (D_p) of the films.

$$D_p = \frac{K\lambda}{\beta_{2\theta} \cos\theta} \quad (1)$$

where K is a constant taken to be 0.94, λ is the wavelength of X-ray used ($\lambda=1.54 \text{ \AA}$) and $\beta_{2\theta}$ is the full width at half maximum, θ is the Bragg angle. The calculated crystallites sizes are shown in Table 1.

Units Morphology Index (MI) is developed from $\beta_{2\theta}$ (FWHM) of XRD data. The $\beta_{2\theta}$ of two peaks are related with MI to its particle morphology. MI is obtained from Equation (2). It correlates with its particle sizes. Details are presented in Table 1.

$$MI = \frac{\beta_h}{\beta_h + \beta_p} \quad (2)$$

where MI is morphology index, β_h is highest β value obtained from peaks and β_p is value of particular peak's β for which MI is to be calculated.

The Lorentz-polarization factor is the most important of the experimental quantities that control X-ray intensity with respect to diffraction angle. In the intensity calculations Lorentz factor is combined with the polarization factor and further the variation of the Lorentz's factor with the Bragg angle (θ) is shown [10-12].

The overall effect of Lorentz factor is to decrease the intensity of reflections at intermediate angles compared to those in the forward and backward directions. Lorentz factor (L_f) and Lorentz polarization factor (LP_f) are calculated from Eqn's (3)

and (4), respectively and tabulated in Table 1.

$$L_f = \frac{\cos\theta}{\sin^2 2\theta} = \frac{1}{4\sin^2\theta \cos\theta} \quad (3)$$

$$LP_f = \left(\frac{1 + \cos^2(2\theta)}{\sin^2\theta \cos\theta} \right) \quad (4)$$

Table: Crystallite sizes (D_p), Morphology index (MI), Lorentz factor (L_f) and Lorentz polarization factor (LP_f) of PNCs.

Electrolytes	2θ	Intensity	D_p (nm)	MI	L_f	LP_f
Pure ZnO NPs	36.22	4037	18.31	1.00	2.721	17.98
PEO/PVP (50:50)	18.98	1455	14.31	0.53	9.332	70.72
PEO/PVP/ZnO (47:47:6)	19.29	436	17.72	0.50	9.038	68.38

Scanning electron microscopy (SEM). The SEM images of PEO/PVP, ZnO and its nanocomposites are shown in Fig. 3. It is evident from the SEM micrograph of ZnO which shows a flower like shape, arranged over one another with narrow size distribution as shown in Fig. 3(a) Fig. 3(b) illustrates PEO/PVP blend observed softer and homogenous in nature. As the content of ZnO increases to 4 wt% the film surface becomes rough with

small particles (white spots) aggregates as shown in Fig 3(c), which indicates homogenous segregation of ZnO in the polymer blend system. Also, this result showed that there is an adhesion between the surface of ZnO NPs and polyblend matrix [13]. Fig. 3(d) gives rise to a coarse spherulitic structure, which is due to the ZnO segregated into interlamellar regions of the blend for 6 wt % of ZnO NPs.

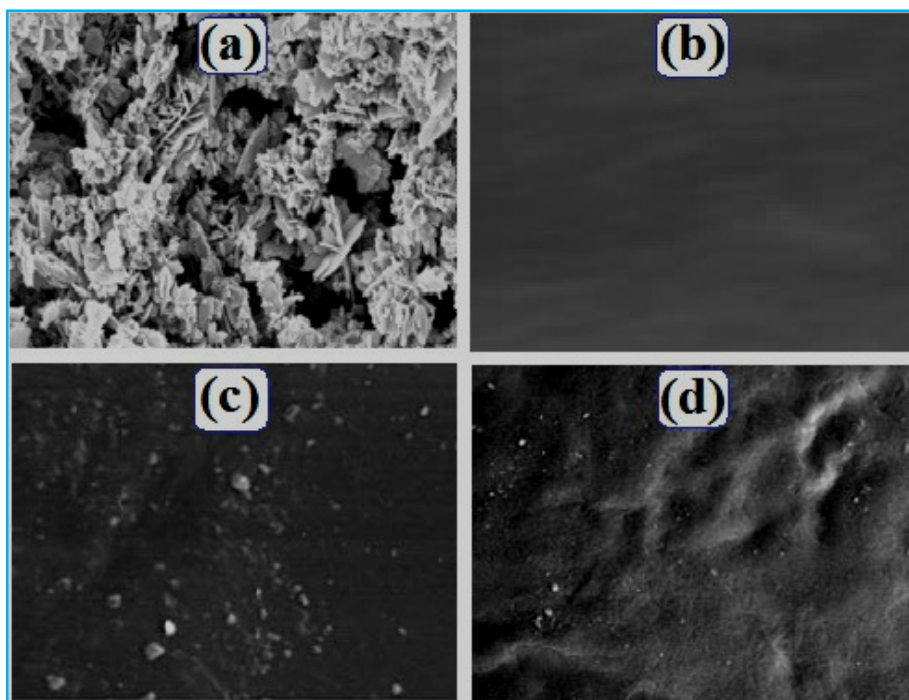


Fig. 3. SEM image of the (a) as-prepared ZnO nanopowder, (b) PEO/PVP blend, (c) 4 and (d) 6 wt% of ZnO PNCs.

Transparency properties. The fundamental absorption edge is one of the most important features of the absorption spectra, which provides the most valuable optical information available for material identification. The nature of optical transition involved

in the blends can be determined on the basis of the dependence of the absorption coefficient (α) on photon energy ($h\nu$). Fig. 4(A) shows the plot of α vs. $h\nu$ for ZnO, PEO/PVP blend films and their electrolyte with different wt% of ZnO NPs.

The values of the absorption edges of ZnO, 4 wt% and 6 wt% PNCs are 4.29, 4.08 and 3.98 eV, respectively. It was observed clearly that the values of the absorption edge for polymer electrolyte decreased as ZnO wt% increases. This indicates the creation of localized states in the band gap as result of the compositional disorder [14].

The reflectance spectra (Fig. 4(B)) showed sharp increases at 386 nm and a material had a strong reflective characteristic after approximately 584 nm for the sample 6 wt% of ZnO NPs doped PEO/PVP blend. This was due to the high possibility of reflectance for the photons lacking the required energy for interacting with electrons or atoms. It was

observed that the absorption of ZnO NPs was strongly affected by the particle sizes. The band gap energies were determined using Kubelka-Munk function.

$$F(R) = \frac{(1-R)^2}{2R} \quad (5)$$

Here (R) is the absolute value of reflectance and F(R) is equivalent to the absorption coefficient [15]. The direct band gap of ZnO and NCs was estimated by plotting $[F(R).hv]^2$ vs. hv (eV). The linear part of the Tauc plot was extrapolated to $[F(R).hv]^2 = 0$ to get the direct band gap energy. The obtained band energy (E_g) values were ZnO is 3.68 eV and 4, 6 wt% of NCs are 4.0 and 3.71eV, respectively.

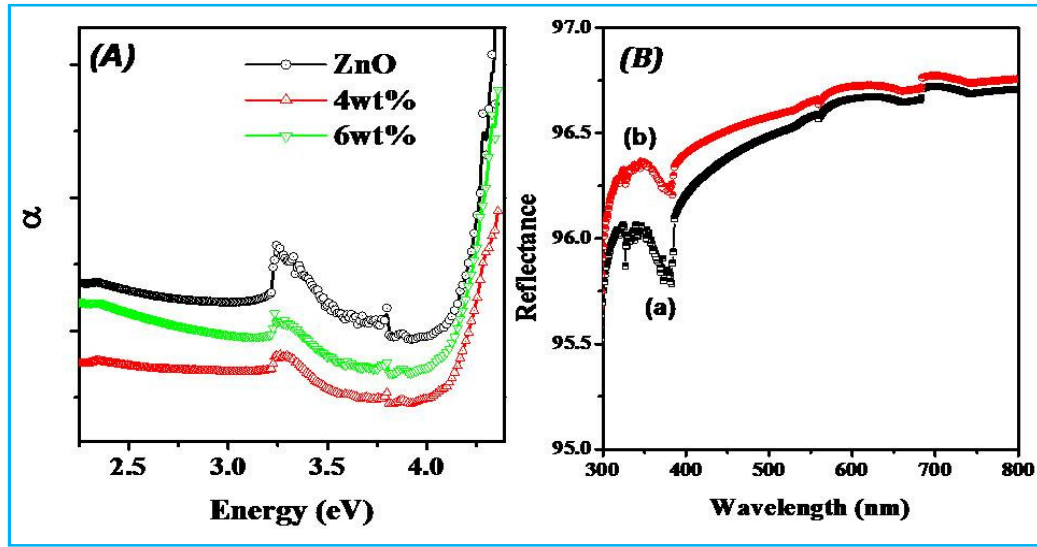


Fig. 4. (A) shows the plot of α vs. hv for ZnO with different concentration of ZnO NPs films and (B) The spectral variation of reflection of the ZnO nanoparticles (a) ZnO NPs and (b) 6 wt% ZnO doped NPs polymer blend electrolytes

Compared to the reported values of bandgap energy of bulk ZnO ($E_g=3.37$ eV) [16], NCs film shows sharp transmission intensity is approximately constant at this value in this wavelength range of 600-800 nm.

Figure 5 shows the variation of skin depth as a function of wavelength for ZnO and NC films. It is a clear from the figure that the skin depth increases as wavelength increases; this behavior could be seen for all samples, but the skin depth decreases as the doping concentration increases, so the skin depth is a transmittance related.

The energy loss is related to the optical property of the material through the dielectric function. The probability that the fast electrons will lose energy while travelling the bulk and the surface of the material is defined as the volume and surface energy loss functions. The energy loss function: volume

energy loss function (VELF) and surface energy loss function (SELF) are related to real and imaginary parts ϵ_1 and ϵ_2 of the complex dielectric constant by the following relation [17].

$$VELF = \frac{\epsilon_2}{\epsilon_1^2 + \epsilon_2^2}, \quad SELF = \frac{\epsilon_2}{(\epsilon_1^2 + 1)^2 + \epsilon_2^2} \quad (6)$$

The variation of these parameters with the photon energy for the ZnO NPs and PNC films is shown in the Fig. 6. It is clear that the volume energy loss is greater than surface energy loss at incident photon energies. It is also clear that the maximum of SELE and VELF correspond to the absorption energy due to the interband. Both a energy losses are when the fast single electrons traverses from valance band to conduction band in the PNC film.

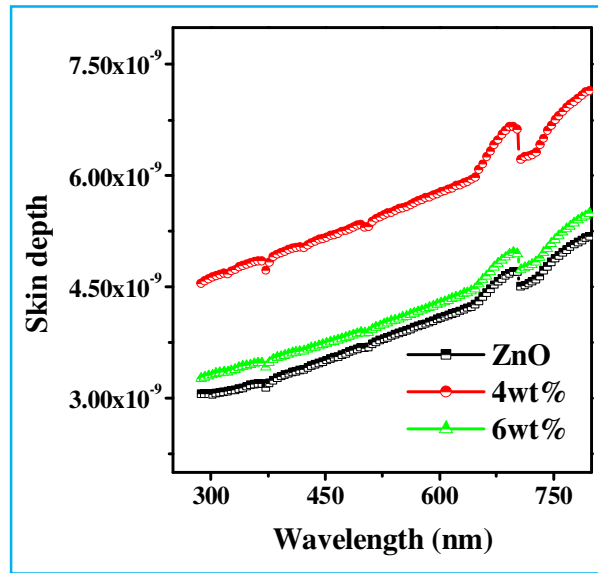


Fig. 5. Plot of skin depth vs. wavelength for ZnO and PNCs.

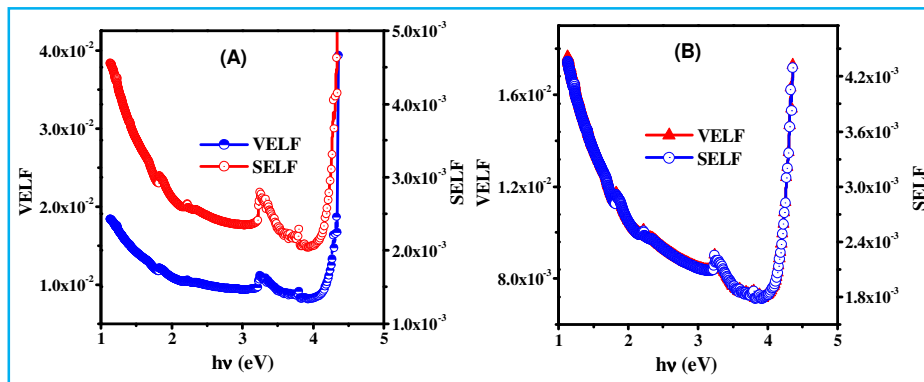


Fig. 6. Volume and surface energy loss functions as a function of photon energy for (A) ZnO NPs and (B) 6 wt% ZnO NPs doped polymer blend electrolyte.

CONCLUSIONS

Synthesis of ZnO NPs by simple Co-precipitation method and ZnO doped PEO/PVP films (PNCs) were deposited on quartz substrate with various wt% using the spin-coat method. XRD analysis reveals the formation of nanostructure films exhibiting hexagonal wurtzite structure with (101) orientation. The optical energy gap and absorption edges values were found to decrease with the rising ZnO wt%. As the dopant increases in polyblend (PEO/PVP) it shows the surface morphology becomes rougher with small white spots and it reveals the tendency towards phase segregation in the interlamellar regions of the polymer chain. Polymer nanocomposites highly transparent spin-coat films are used in optical devices.

ACKNOWLEDGEMENTS

The authors are grateful to UGC-New Delhi, for sanctioning the research project (F.No. 41-879/2012/SR dated 25-07-2012).

REFERENCES

- [1] J.E. Bauerle, "Study of solid electrolyte polarization by a complex admittance method", *J Phys Chem Solids*, Vol. **30**, 1969 Pg. 2657–2670.
- [2] K. Kesavan, S. Rajendran, C.M. Mathew, "Influence of Barium Titanate on poly(vinyl pyrrolidone)-based composite polymer blend electrolytes for lithium battery applications" *Polymer Composites*, Vol. **36**, 2015, Pg. 302–311.
- [3] L.A. Utracki, "Polymer Alloys and Blends: Thermodynamics and Rheology", Hanser Gardner Publications, 1990 – Science, pages 367.

- [4] M. R. Johan, O. O. Shy, S. Ibrahim, S. M. M. Yassin and T. Y. Hue, "Effects of Al_2O_3 Nanofiller and EC Plasticizer on the Ionic Conductivity Enhancement of Solid PEO-LiCF₃SO₃ Solid Polymer Electrolyte", *Solid State Ionics*, Vol. **196**, 2011, Pg. 41-47.
- [5] S. Radhakrishnan, P.D. Venkatachalapathy, "Effect of Casting Solvent on the Crystallization in PEO/PMMA Blends", *Polymer*, Vol. **37**, 1996, Pg. 3749–3752.
- [6] D. A. J. Rand, "Battery systems for electric vehicles — a state-of-the-art review", *J Power Sources*, Vol. **4**, 1979. Pg. 101–143.
- [7] Sharanappa Chapi and Devendrappa H., "Enhanced electrochemical, structural, optical, thermal stability and ionic conductivity of (PEO/PVP) polymer blend electrolyte for electrochemical applications", *Ionics*, Vol. **22**, 2016, Pg. 803–814.
- [8] A.P. Rambu, D. Sirbu, A.V. Sandu, G. Prodan, V. Nica, "Influence of In doping on electro-optical properties of ZnO films", *Bull Mater Sci*, Vol. **36**, 2013, Pg. 231–237.
- [9] R. Kripala, A. K. Gupta, R. K. Srivastava, S. K. Mishra, "Photoconductivity and photoluminescence of ZnO nanoparticles synthesized via co-precipitation method", *Spectrochimica Acta Part A*, Vol. **79**, 2011, Pg. 1605–1612.
- [10] H. S. Peiser, H. P. Rooksby and A. J. C. Wilson, "X-Ray Diffraction by Polycrystalline Materials," The Institute of Physics, London, 1955.
- [11] G. L. Clark, *Applied X-Rays*, 4th Edition, McGraw- Hill Book Company, Inc., New York, 1955.
- [12] A.H. Compton, S. K. Allison, *X-Rays in Theory and Experiment*, D. Van Nostrand Company, Inc., New York, 1935.
- [13] A. Matei, I. Cernica, O. Cadar, C. Roman, V. Schiopu, "Synthesis and characterization of ZnO – polymer nanocomposites", *Int J Mater Form*, Vol. **1**, 2008, Pg. 767–770.
- [14] O.Gh. Abdullah, B.K. Aziz, S.A. Hussen, "Optical Characterization of Polyvinyl alcohol – Ammonium Nitrate Polymer Electrolytes Films", *Chemical and Material Research*, Vol. **3**, 2013, Pg. 84-90.
- [15] M. R. Parra, F. Z. Haque, "Aqueous chemical route synthesis and the effect of calcination temperature on the structural and optical properties of ZnO nanoparticles", *J Mater Res Technol*, Vol. **3**, 2014, Pg. 363–369.
- [16] D. Li, J. Hu, F. Fan, S. Bai, R. Luo, A. Chen, C.C Liu, "Quantum-sized ZnO nanoparticles synthesized in aqueous medium for toxic gases detection", *J Alloys Compd*, Vol. **539**, 2012, Pg. 205–209.
- [17] S. Sarkar, N.S. Das, K.K. Chattopadhyay, "Optical constants, dispersion energy parameters and dielectric properties of ultra-smooth nanocrystalline BiVO₄ thin films prepared by rf-magnetron sputtering", *Solid State Sciences*, Vol. **33**, 2014, Pg. 58–66.